JOURNAL OF CATALYSIS 79, 203–206 (1983)

The Structure and Properties of Tungsten Oxide on Silica and on Alumina

High-resolution transmission electron microscopy (TEM) has been used to determine the size of metal clusters on oxide supports (*1–3*). When chemisorption studies are coupled with electron microscopy, it is sometimes possible to assign "raft" configurations to these clusters and establish the thickness of the "raft" to be one layer (*2, 4*). In an analogous fashion the morphology of WO_3 on SiO_2 was investigated by TEM combined with chemisorption of *n*-butylamine on the exposed W^{6+} acid sites.

A WO_3 on SiO_2 (300 m^2/g) sample was prepared by the incipient wetness impregnation method using ammonium *meta*-tungstate followed by drying at 110°C and calcination at 500°C. For tungsten concentrations on SiO_2 below 5 wt%, the electron micrographs show clusters of WO_3, a polymeric tungsten oxide phase, with a narrow distribution of diameters about a mean of 1.2 nm (Fig. 1). Thus, it is clear that the 12-unit ammonium *meta*-tungstate polyanion has decomposed during drying and calcining to give much smaller WO_3 clusters. This observation is a unique example of a supported oxide with a cluster size distribution that is in the range of well dispersed noble metal catalysts (*4, 5*).

A one-to-one correspondence of the acid sites with WO_3 content, i.e., one acid site for *every* WO_3 introduced (below 5 wt%), was established by chemisorption of *n*-butylamine on samples of WO_3 on SiO_2 (*6–9*). The acid sites must therefore be present in the small WO_3 clusters or in the SiO_2 support immediately surrounding the WO_3 clusters.

For >5 and <20 wt% WO_3 on SiO_2 a bimodal distribution of cluster sizes was observed. For example, the number density and size of the small clusters observed on the surface of a 20 wt% WO_3 on SiO_2 sam-

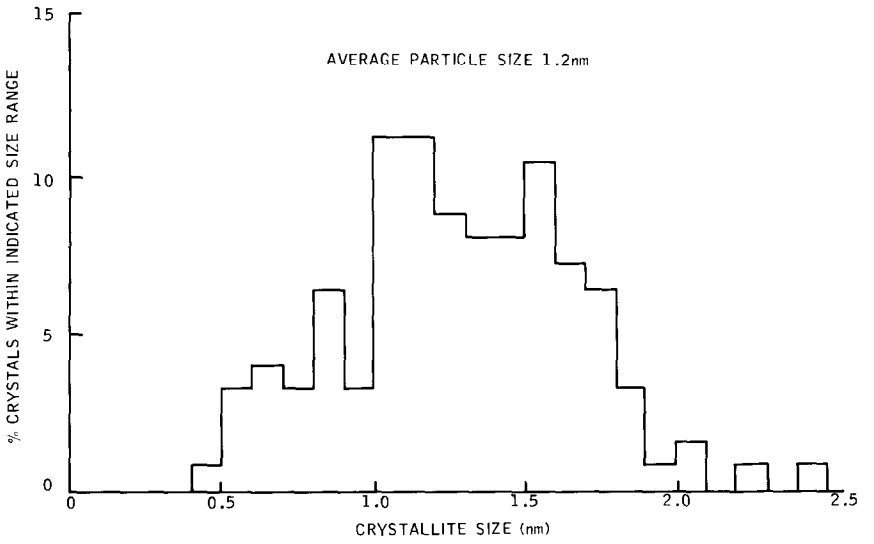

FIG. 1. Particle size distribution of 2.3 wt% tungsten oxide on silica.

0021-9517/83/010203-04$03.00/0

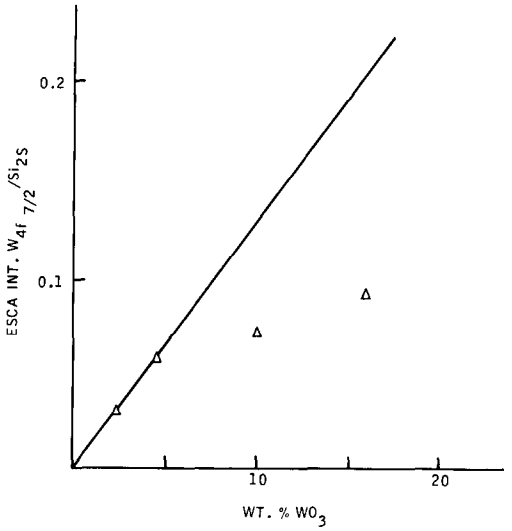

FIG. 2. ESCA W_{4f}/Si_{2S} intensity ratio as a function of the WO_3 content of WO_3 on SiO_2.

ple were similar to those seen on a 5 wt% sample. Three quarters of the WO_3 in the 20% sample, however, was present as 10–15 nm particles as observed by X-ray powder scans and electron microscopy. This bimodal distribution was substantiated by ESCA W/Si intensity ratio studies (*10, 11*) as a function of WO_3 content. We observed a linear increase of the $W_{4f_{7/2}}$-to-Si_{2S} intensity ratio with tungsten content up to 5 wt% WO_3 and then the ratio deviated considerably from linearity with increasing tungsten content (see Fig. 2). The number of acid sites also increased linearly with WO_3 content until the large clusters began to form (see Fig. 3). After that point, the number of acid sites remained constant, independent of the WO_3 content.

The bimodal distribution of WO_3 clusters on SiO_2 above 5 wt% WO_3 content suggests that there are a limited number of sites on the SiO_2 surface which can interact with small WO_3 clusters and that, above that limit, WO_3 aggregates into a crystalline WO_3 phase. The strong interaction of WO_3 and an Al_2O_3 surface has recently been reported (*12*). This interaction may result in the formation of unique materials when WO_3 and Al_2O_3 are simultaneously supported on SiO_2. These supported mixed oxides were made by coimpregnation of aluminum nitrate and ammonium *meta*-tungstate in water by the incipient wetness method. The samples were then dried at 120°C and calcined at 500°C for 16 hr. For these samples there was a linear relationship between the W-to-Si ESCA intensity ratio and the tungsten content for all levels of W loading (see Fig. 4). Also, TEM failed to detect WO_3 clusters observed when WO_3 alone was supported on SiO_2. This was the case even at high WO_3 and low Al_2O_3 loadings. Apparently, alumina incorporation onto the silica surface results in a large number of sites where WO_3 interacts so strongly that formation of clusters or particles of WO_3 is precluded. Distinct analogies are apparent for these WO_3–

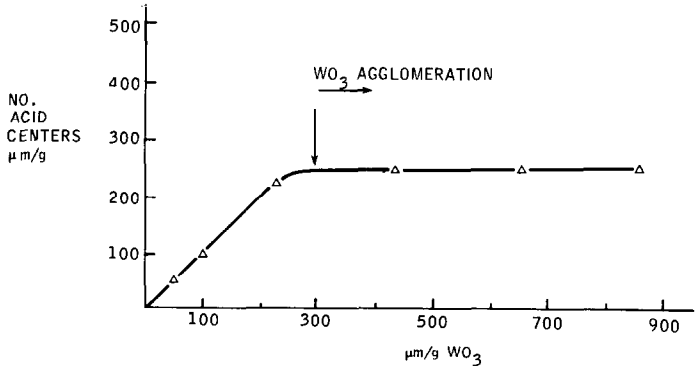

FIG. 3. Relationship of number of acid centers (μmole/g) measured by butylamine titration and the WO_3 concentration (μmole/g) for WO_3 on SiO_2.

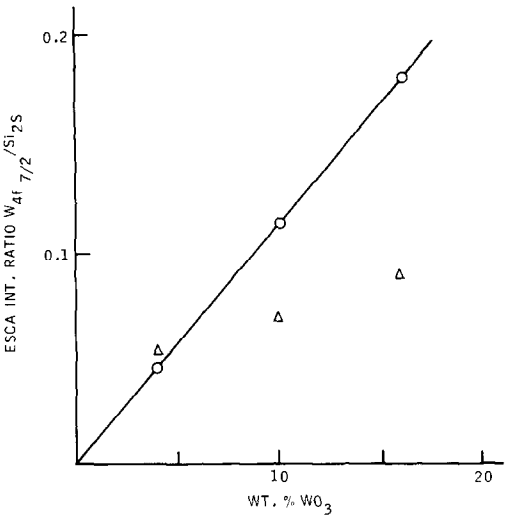

FIG. 4. ESCA W_{4f}/Si_{2S} intensity ratio as a function of the WO_3 content of WO_3 and Al_2O_3 mixed oxides dispersed onto a SiO_2 support. Total supported mixed oxide content (WO_3 + Al_2O_3) of 20 wt%.

Al_2O_3 on SiO_2 systems and WO_3 on γ-Al_2O_3 itself (*vide infra*).

High-resolution transmission electron microscopy studies of tungsten oxide on γ-Al_2O_3 (180 m^2/g) show no detectable structure of the supported phase even at high surface coverage (25 wt% WO_3). Similar results have been reported by Delannay (*13*) for 15 wt% MoO_3 on Al_2O_3. When a 10 wt% WO_3 on Al_2O_3 sample was steamed in air (air sparged through water at 500 cm^3/min) at 900°C to reduce the surface area to 70 m^2/g no agglomerated WO_3 phase or small clusters could be detected by TEM. Ten weight percent WO_3 represents about monolayer coverage of the 70 m^2/g of surface area. An ESCA study of the W surface concentration showed a linear increase in the W/Al ratio with W content up to 10 wt% for a series of steamed samples. This result suggests an increase in WO_3 surface concentration as the alumina surface area collapses. Apparently, there is a very strong interaction between WO_3 and Al_2O_3 (*12*) which precludes cluster formation which is so predominant in the case of WO_3 on SiO_2 even at low WO_3 concentrations. Even in the case of a 25 wt% sample treated under analogous conditions where the surface area was again reduced to 70 m^2/g *no small clusters* could be detected. Large 15 nm particles of WO_3 were formed as the support surface area collapsed. The final state of this 25% sample was a bimodal distribution of a highly dispersed amorphous phase and large particles of crystalline WO_3.

EXAFS studies to determine the structure of WO_3 on SiO_2 and on γ-Al_2O_3 supports are in progress. On a 2.3 wt% WO_3 on SiO_2 sample, with 1.2 nm WO_3 clusters observed by TEM, both W–O bonds and a W–O–W bond have been identified. For WO_3 on γ-Al_2O_3, W–O bonds have also been identified, but no W–O–W bond has been observed. When the EXAFS and TEM results are considered together, it appears that isolated or randomly positioned WO_3 units are "locked" into the alumina hydroxyl structure of the Al_2O_3. Even a severe steam treatment of WO_3 on γ-Al_2O_3, which causes significant collapse of the alumina surface area, fails to form detectable three-dimensional particles unless the monolayer coverage limit is exceeded. In recent work by Hercules and co-workers (*14*) monolayer coverage of WO_3 on γ-Al_2O_3 was determined to occur at a loading of 24 wt% WO_3. Above 15 wt% WO_3 Raman spectroscopy studies suggests the WO_3 to be present as "an octahedral WO_3-like interaction species" (*14*). Our EXAFS and TEM results are not necessarily inconsistent with this proposal as the "octahedral WO_3-like species" may not be detectable by the present techniques, or this species may *not* be a "polymeric" phase.

ACKNOWLEDGMENTS

The authors would like to acknowledge the excellent experimental work by N. C. Dispenziere, Jr. in the course of these studies.

REFERENCES

1. Prestridge, E. B., and Yates, D. J. C., *Nature (London)* **234**, 345 (1971).
2. Yates, D. J. C., Murrell, L. L., and Prestridge, E. B., *J. Catal.* **57**, 41 (1979).

3. Baker, R. T. K., Prestridge, E. B., and Garten, R. L., *J. Catal.* **59,** 293 (1979).
4. Yates, D. J. C., Murrell, L. L., and Prestridge, E. B., *in* "Growth and Properties of Metal Clusters" (J. Bourdon, ed.), Elsevier, Amsterdam, 1980.
5. Yates, D. J. C., and Sinfelt, J. H., *J. Catal.* **8,** 348 (1967).
6. The *n*-butylamine adsorption technique employed dry box techniques using the Benesi method as reported previously (*7*) combined with ultrasonic treatment of the samples (65°C) for 10 min between butylamine additions to ensure equilibration (8). Dicinnamalacetone, benzalacetophenone, and anthraquinone indicator solutions were added to small aliquots of the titrated slurry to establish the titration endpoint. This procedure has been shown in our laboratory to provide acid center distributions very similar to those obtained by the standard Benesi method (*9*). Silica had zero acidity as measured by the above series of indicators.
7. Reitsma, H. J., and Boelhouwer, C., *J. Catal.* **33,** 39 (1974).
8. Bertolacini, R. J., *Anal. Chem.* **35,** 599 (1963).
9. Benesi, H. A., *J. Amer. Chem. Soc.* **78,** 5490 (1956).
10. Angevine, J. P., Delgass, W. N., and Vartuli, J. C., *Proc. Sixth Int. Conr. Catal.* **2,** 611 (1976).
11. Fung, S. C., *J. Catal.* **58,** 454 (1979).
12. Thomas, R., Kerkkof, F. P. J. M., Moulijn, A. J., Medema, J., and DeBeer, V. H. J., *J. Catal.* **61,** 559 (1980).
13. Delannay, F., *Catal. Rev-Sci. Eng.* **22,** 141 (1980).
14. Salvate, L., Jr., Makovsky, L. E., Stencel, J. M., Brown, F. R., and Hercules, D. M., *J. Phys. Chem.* **85,** 3700 (1981).

L. L. MURRELL
D. C. GRENOBLE
R. T. K. BAKER
E. B. PRESTRIDGE
S. C. FUNG
R. R. CHIANELLI
S. P. CRAMER

Corporate Research
Exxon Research and Engineering Co.
P. O. Box 45
Linden, New Jersey 07036

Received February 24, 1982; revised August 23, 1982